

A Novel Integrated Control Strategy for a Cost-effective Inverted Pendulum System with Camera-based Observation

Ngoc-Khoat Nguyen

Faculty of Control and Automation, Electric Power University, Hanoi, Vietnam
khoatnn@epu.edu.vn (corresponding author)

Thi-Mai-Phuong Dao

Faculty of Automation, School of Electrical and Electronic Engineering (SEEE), Hanoi University of Industry, Hanoi, Vietnam
daophuong@hau.edu.vn

Van-Hung Pham

Faculty of Automation, School of Electrical and Electronic Engineering (SEEE), Hanoi University of Industry, Hanoi, Vietnam
hungphamvan@hau.edu.vn

Tien-Dung Nguyen

Faculty of Control and Automation, Electric Power University, Hanoi, Vietnam
dungnt@epu.edu.vn

Thi-Kim-Thanh Tran

Practical and Experiment Center, Electric Power University, Hanoi, Vietnam
thanhttk@epu.edu.vn

Van-Tien Nguyen

Technical Department, Petro Electric Energy Joint Stock Company, Hanoi, Vietnam
tien11a.k8@gmail.com

Received: 14 February 2025 | Revised: 10 March 2025 | Accepted: 19 March 2025

Licensed under a CC-BY 4.0 license | Copyright (c) by the authors | DOI: <https://doi.org/10.48084/etasr.10581>

ABSTRACT

To improve the ability to control the balance of an inverted pendulum on a cart system, a refined fuzzy logic inference approach using the Sugeno model is introduced. This new approach leverages the capabilities of the ESP32 CAM and YOLO v3. The ESP32 CAM provides real-time image and video capture, whereas YOLO v3, operating on a more robust processing platform, performs object detection within the captured data. This integration of image processing and object recognition necessitates a complex experimental setup, requiring further refinement of the adaptable robotic model and integration of various techniques. A WinForms interface has been developed for the control and monitoring of the camera-equipped inverted pendulum system. This interface allows the users to monitor and adjust the system parameters, as well as to visualize the surrounding environment. This design significantly enhances the sophistication of the control and monitoring system while maintaining cost-effectiveness. Numerical simulations and experimental results demonstrate markedly improved control performance, validating the novel integrated control methodology.

Keywords-inverted pendulum system; observation; image processing; YOLOv3; integrated control methodology

I. INTRODUCTION

The inverted pendulum model serves as a canonical example of a mechatronic system, consisting of a vertically oriented rod (the pendulum) affixed to a movable base referred to as a cart. The primary objective is to maintain the pendulum in an upright position by precisely regulating the cart's motion. This system presents a highly complex nonlinear control challenge due to the intricate interdependencies among the pendulum's angular displacement, the cart's position, and the external forces acting on the system. The inherent instability and nonlinearity of the inverted pendulum makes it an essential platform for research and education in automatic control, providing a rigorous theoretical foundation for the development and analysis of various control strategies. Additionally, this model finds extensive applications in fields such as multipurpose robotics, self-balancing vehicles, and stability control systems [1, 2].

Several studies have investigated the control of inverted pendulum systems. Authors in [3] compared various control strategies, including Proportional-Integral-Derivative (PID), fuzzy logic, neural networks, and Linear Quadratic Regulator (LQR), and found that Fuzzy Logic Controllers (FLCs) outperformed the others in stabilizing the system. Authors in [4] explored a hybrid fuzzy-PID controller for a rotary pendulum system, demonstrating improved performance over either PID or fuzzy controllers alone. Authors in [5] proposed a Lyapunov-based controller for an inverted pendulum vehicle system. In another application, authors in [6] used the ESP32 CAM module with Google Lens technology to detect and read vehicle license plates. This demonstrated the image processing and object recognition capabilities of the ESP32 CAM platform. Building on this, authors in [7] showed how ESP32 CAM can detect driver drowsiness by analyzing facial images. Authors in [8] focused on creating a mathematical model and control algorithms for the inverted pendulum system. In another study, authors in [9] utilized Python's OpenCV library with the YOLO v3 algorithm to process ESP32 CAM images, enabling object detection and recognition. Furthermore, authors in [10] explored image processing techniques in Python, highlighting the importance of libraries like OpenCV and NumPy. Several studies have also explored the integration of image processing and object recognition. For example, authors in [11] used image processing to evaluate fish freshness by analyzing gill tissue characteristics. Other studies, such as those presented in [12-19], have examined diverse control methodologies for inverted pendulum systems, encompassing PID control, fuzzy logic control, LQR design, and optimization-based approaches. However, most of these investigations have prioritized system control mechanisms without incorporating image processing and object recognition capabilities.

The main contributions of the current paper include the design and implementation of an inverted pendulum vehicle system. This system employs a Sugeno PD-based fuzzy logic control architecture, utilizing a Modified Genetic Algorithm (MGA), adapted from the methodology described in [1], to ensure dynamic equilibrium. In addition, the system integrates an ESP32 CAM observation camera for comprehensive

environmental monitoring and object recognition. Image processing techniques, coupled with the YOLO v3 algorithm, are employed for accurate object detection and identification. A dedicated monitoring interface provides real-time system status information and facilitates the observation and identification of objects within the acquired image data.

This research uniquely integrates advanced control methodologies, sophisticated image processing capabilities, and robust object recognition algorithms within a unified platform. This synergistic approach presents significant potential for diverse applications, including service robotics, autonomous transportation systems, and advanced security surveillance systems.

II. THE TYPICAL MODEL OF A CART-INVERTED PENDULUM SYSTEM UNDER STUDY

Consider an inverted pendulum model mounted on a small cart moving in a straight line, as shown in Figure 1. Neglect the friction between the cart and the road as well as the friction between the cart and the pendulum. The system parameters include M - the mass of the car; m - the mass of the pendulum (including a camera as proposed in this study); l - the length of the rod; θ - the angle formed by the rod with the vertical plane; F - the control force; x - the position of the pendulum; g - the acceleration due to gravity.

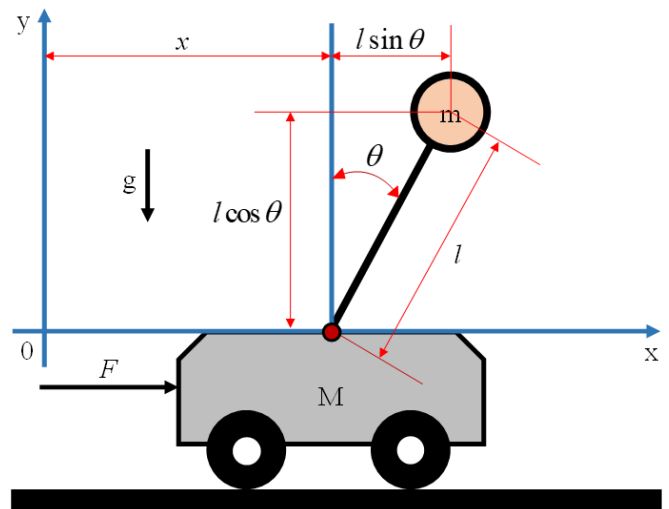


Fig. 1. The dynamic model of an inverted pendulum cart system.

There are many methods to mathematically model the inverted pendulum system, among which the Euler-Lagrange method [8, 20] is considered due to its popularity, regularity, and simplicity. The Lagrange equation is as follows:

$$\frac{d}{dt} \left(\frac{\partial L}{\partial \dot{\theta}_k} \right) - \frac{\partial L}{\partial \theta_k} = F_k \quad (1)$$

where:

- $L = T - V$ is the Lagrangian operator.
- T is the total kinetic energy of the system.

- V is the total potential energy of the system.
- θ_k is the generalized coordinate.
- F_k is the total external force acting on the system (moment).

The parameters θ_k and F_k are expressed as follows:

$$\theta_k = \begin{bmatrix} x \\ \theta \end{bmatrix}; F_k = \begin{bmatrix} F \\ \theta \end{bmatrix} \quad (2)$$

Since the reference point for the potential energy is chosen at $y = 0$, the potential energy of the cart is always zero, and the potential energy of the system is the potential energy of the pendulum V :

$$V = mgy_k = mgl \cos(\theta) \quad (3)$$

The kinetic energy of the cart T_1 is:

$$T_1 = \frac{1}{2} M \dot{x}^2 \quad (4)$$

The position of the pendulum projected onto the coordinate system is:

$$\begin{cases} x_k = x + l \sin(\theta) \\ y_k = l \cos(\theta) \end{cases} \quad (5)$$

The derivative of the pendulum's position is the velocity of the pendulum in the coordinate system:

$$\begin{cases} v_{xk} = \dot{x} + l \dot{\theta} \cos(\theta) \\ v_{yk} = -l \dot{\theta} \sin(\theta) \end{cases} \quad (6)$$

The square of the pendulum's average velocity v is:

$$v^2 = v_{xk}^2 + v_{yk}^2 = \dot{x}^2 + 2l\dot{x}\dot{\theta} \cos(\theta) + l^2 \dot{\theta}^2 \quad (7)$$

Thus, the kinetic energy of the pendulum T_2 is:

$$T_2 = \frac{1}{2} m v^2 = \frac{1}{2} m \dot{x}^2 + m l \dot{x} \dot{\theta} \cos(\theta) + \frac{1}{2} m l^2 \dot{\theta}^2 \quad (8)$$

Therefore, the total kinetic energy T of the system is:

$$T = T_1 + T_2 = \frac{1}{2} M \dot{x}^2 + \frac{1}{2} m \dot{x}^2 + m l \dot{x} \dot{\theta} \cos(\theta) + \frac{1}{2} m l^2 \dot{\theta}^2 \quad (9)$$

Thus, the Euler-Lagrange equation is as follows:

$$L = T - V = \frac{1}{2} M \dot{x}^2 + \frac{1}{2} m \dot{x}^2 + m l \dot{x} \dot{\theta} \cos(\theta) + \frac{1}{2} m l^2 \dot{\theta}^2 - mgl \cos(\theta) \quad (10)$$

where:

$$\begin{cases} \frac{\partial L}{\partial \dot{x}} = (m + M) \dot{x} + m l \dot{\theta} \cos(\theta) \\ \frac{d}{dt} \left(\frac{\partial L}{\partial \dot{x}} \right) = (m + M) \ddot{x} + m l \ddot{\theta} \cos(\theta) - m l \dot{\theta}^2 \sin(\theta) \\ \frac{\partial L}{\partial x} = 0 \\ \frac{\partial L}{\partial \dot{\theta}} = m l \dot{x} \cos(\theta) + m l^2 \dot{\theta} \\ \frac{d}{dt} \left(\frac{\partial L}{\partial \dot{\theta}} \right) = m l [\ddot{x} \cos(\theta) - \dot{x} \dot{\theta} \sin(\theta)] + m l^2 \ddot{\theta} \\ \frac{\partial L}{\partial \theta} = mgl \sin(\theta) - m l \dot{x} \dot{\theta} \sin(\theta) \end{cases} \quad (11)$$

By substituting into the Euler-Lagrange equations, we obtain the following equations for the inverted pendulum on a cart system:

$$\begin{cases} (m + M) \ddot{x} + m l \ddot{\theta} \cos(\theta) - m l \dot{\theta}^2 \sin(\theta) = F \\ m l \ddot{x} \cos(\theta) + m l^2 \ddot{\theta} - mgl \sin(\theta) = 0 \end{cases} \quad (12)$$

Solving for \ddot{x} and $\ddot{\theta}$ step-by-step, one can be obtained as follows:

$$\begin{cases} \ddot{x} = \frac{F + m l \dot{\theta} \sin(\theta) - m g \cos(\theta) \sin(\theta)}{m + M - m \cos^2(\theta)} \\ \ddot{\theta} = \frac{F \cos(\theta) + m l \dot{\theta}^2 \cos(\theta) \sin(\theta) - (m + M) g \sin(\theta)}{l(m + M - m \cos^2(\theta))} \end{cases} \quad (13)$$

The nonlinear model delineated in (13) serves as a canonical representation for the cart-inverted pendulum system. This mathematical model is then implemented in the MATLAB/Simulink environment to facilitate the application of a novel control strategy proposed in this study.

III. DESIGN OF AN INTEGRATED CONTROL STRATEGY FOR THE INVERTED PENDULUM SYSTEM

This section presents a novel integrated control methodology for stabilizing an inverted pendulum cart system equipped with a camera. In applications involving nonlinear or complex systems, such as the inverted pendulum system under the current study, FLCs often outperform traditional PID controllers. This advantage is due to the fact that, unlike PID controllers, FLCs do not depend on an exact mathematical model of the system. Instead, they utilize linguistic rules and fuzzy sets to manage uncertainty and imprecision, effectively simulating human-like decision making. As a result, FLCs exhibit greater adaptability to dynamic conditions and enhanced resilience against disturbances. Furthermore, FLCs can be designed to integrate expert knowledge or heuristics, further improving their effectiveness in specific applications [21, 22].

The system employs a PD-type FLC optimized with the MGA biomimetic algorithm, a further improved fuzzy inference with the Sugeno mechanism (in previous work, authors in [1] applied the Mamdani inference model). The

Sugeno model may have more effective features than the Mamdani model, realized on the inverted pendulum system [22]. To enhance system functionality, a camera is incorporated into the hardware configuration to enable observation and tracking of target objects. Consequently, the system integrates the ESP Cam, Yolo V3, and a WinForms interface to ensure its versatility. The following subsections provide a detailed description of this integrated control strategy.

A. PD-type Sugeno Fuzzy Logic Controller with Modified Genetic Algorithm

This subsection presents a suitable control architecture for the inverted pendulum model. The proposed control architecture mirrors conventional fuzzy logic control, with a key divergence: the utilization of an MGA to optimize pre- and post-processing coefficients within the fuzzy inference stage, as described in [1]. In contrast to the Mamdani-type fuzzy inference used in our previous study; a Sugeno-type fuzzy inference is used in the current research. Figure 2 depicts the 2-input/1-output PD Sugeno-type fuzzy logic control structure, implemented in the MATLAB/Simulink environment.

Although both the Mamdani-type and Sugeno-type fuzzy logic architectures share fundamental operational principles, subsequent simulations and real-world experiments on the inverted pendulum model will clearly demonstrate the superior suitability and enhanced control performance achieved by implementing the Sugeno-type fuzzy logic model. The proposed fuzzy logic architecture has two input variables: (1) deviation angle which is fuzzified into 7 sets {NB, NM, NS, ZE, PS, PM, PB}, and angular velocity which is also fuzzified into 7 similar sets {NB, NM, NS, ZE, PS, PM, PB}. The output variable of the fuzzy controller is PWM (Pulse Width Modulation) which is fuzzified into 7 level sets {NB, NM, NS, ZE, PS, PM, PB}. The proposed FLC employs triangular membership functions for the output, consistent with the Sugeno model, as shown in Figure 2. A rule base of 49 fuzzy rules, detailed in Table I, provides comprehensive coverage of control scenarios for the inverted pendulum system.

TABLE I. FUZZY LOGIC RULES FOR THE PROPOSED FLC

		Angular velocity						
		NB	NM	NS	ZE	PS	PM	PB
Deviation angle	NB	NB	NB	NB	NB	NB	NM	ZE
	NM	NB	NB	NB	NB	NM	ZE	PM
	NS	NB	NB	NB	NM	ZE	PM	PB
	ZE	NB	NB	NM	ZE	PM	PB	PB
	PS	NB	NM	ZE	PM	PB	PB	PB
	PM	NM	ZE	PM	PB	PB	PB	PB
	PB	ZE	PM	PB	PB	PB	PB	PB

B. Programming ESP32 CAM with Python OpenCV Yolo V3 for Object Detection and Recognition

In this work, a static IP configuration program was first uploaded to the ESP32 CAM module to obtain the camera's static IP address. Next, a directory containing the necessary files for object recognition was created using Yolo V3 in Python. The downloaded Yolo V3 files, including coco.names,

yolov3.cfg, yolov3.weights, were placed in the newly created directory along with the main Python programming file, as shown in Figure 3. The Python program [23] connects to the ESP32 CAM, uses Yolo V3 to detect and recognize objects in images from the camera, and then transmits this image information to the WinForms interface for user monitoring. Image information is transmitted between WinForms and Python via TCP. The static IP address of the ESP32 CAM is displayed on the screen, and for this study, the static IP address was set to '192.168.0.103', as shown in Figure 4.

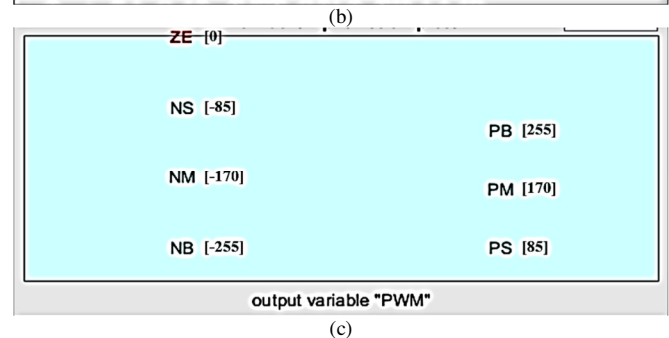
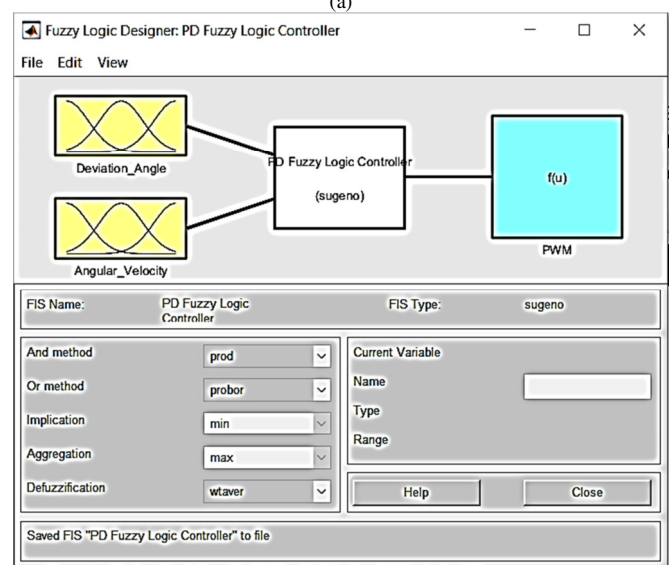
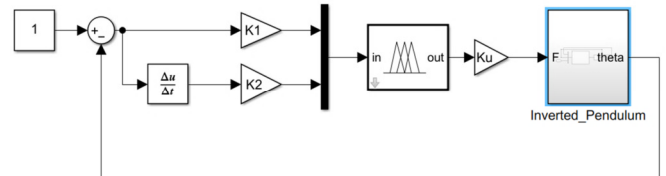


Fig. 2. PD-type FLC based on the Sugeno mechanism built on the MATLAB/Simulink environment: (a) FLC structure in Simulink, (b) Sugeno inference model in detail, and (c) PWM output of the proposed FLC with 7 logic levels.

C. Building a Monitoring Interface for the System

The control and monitoring interface for the entire inverted pendulum system with an attached camera, shown in Figure 5, allows users to track and control system parameters. This interface displays key parameters such as the pendulum's

deviation angle and motor control pulses, as well as image information from the camera, enabling users to observe the surrounding environment. The interface also includes real-time graphs of the pendulum's deviation angle and motor control pulses. The deviation angle graph allows users to monitor the pendulum's stability during operation. The motor control pulse graph helps users control the force applied to the system to maintain balance.

This WinForms interface connects to and receives real-time data from the Arduino Mega 2560 system. Parameters such as deviation angle and motor control pulses are transmitted from the Arduino to WinForms via UART communication. Simultaneously, WinForms also sends control parameters to the Arduino via UART to control the inverted pendulum system.

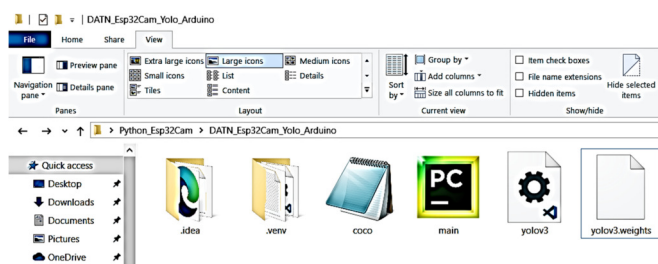


Fig. 3. Directory containing the necessary files.

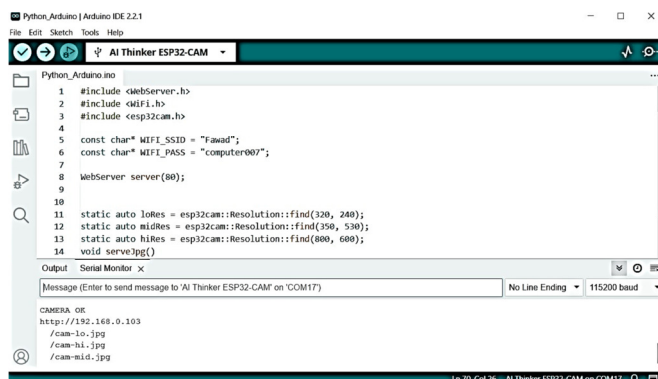


Fig. 4. The IP address of the ESP32 CAM integrated in the inverted pendulum system.

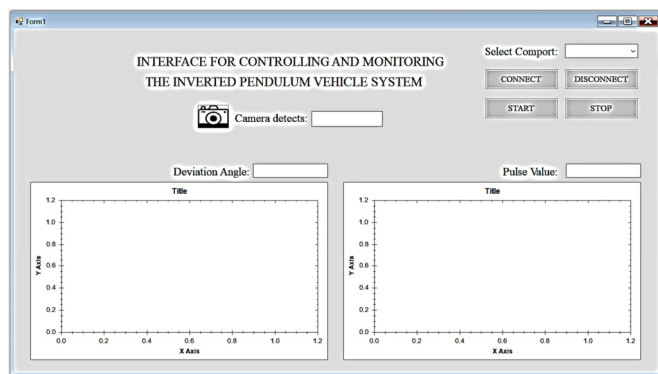


Fig. 5. Design of the control monitoring interface for the entire system.

IV. SIMULATION AND EXPERIMENTAL RESULTS

To rigorously validate the performance of the integrated multi-purpose self-balancing inverted pendulum control system presented in this study, a comprehensive evaluation encompassing both simulation and experimental validation is required. MATLAB/Simulink was selected as the simulation platform. The fundamental simulation parameters include $m = 0.5$ kg; $M = 2$ kg; $l = 1$ m and $g = 9.81$ m/s². For comparative analysis, three distinct control strategies were implemented to regulate the angular displacement of the pendulum: a traditional PID controller, a Mamdani-type fuzzy PD controller as detailed in [1], and a novel Sugeno-type fuzzy PD controller augmented with the proposed MGA optimization algorithm [1]. Simulations were conducted in MATLAB, employing each controller under an initial condition of a -1 radian pendulum deflection angle (θ). The results, displayed graphically in Figure 6, confirm the effective stabilization of the inverted pendulum around its vertical equilibrium position.

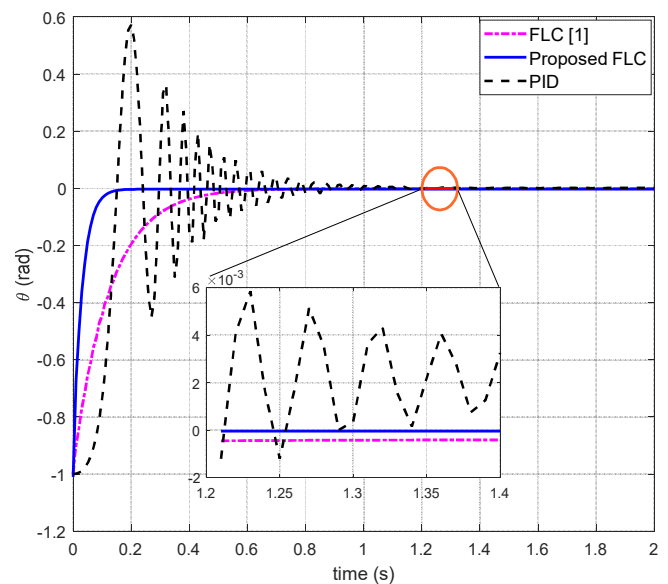
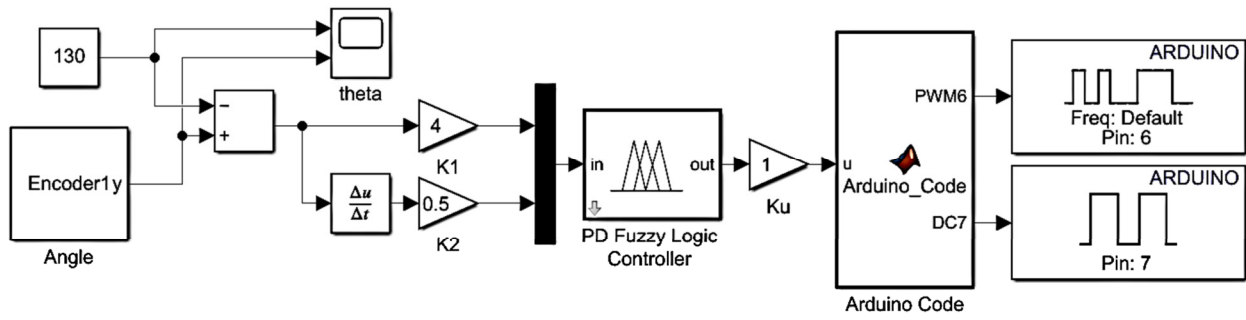


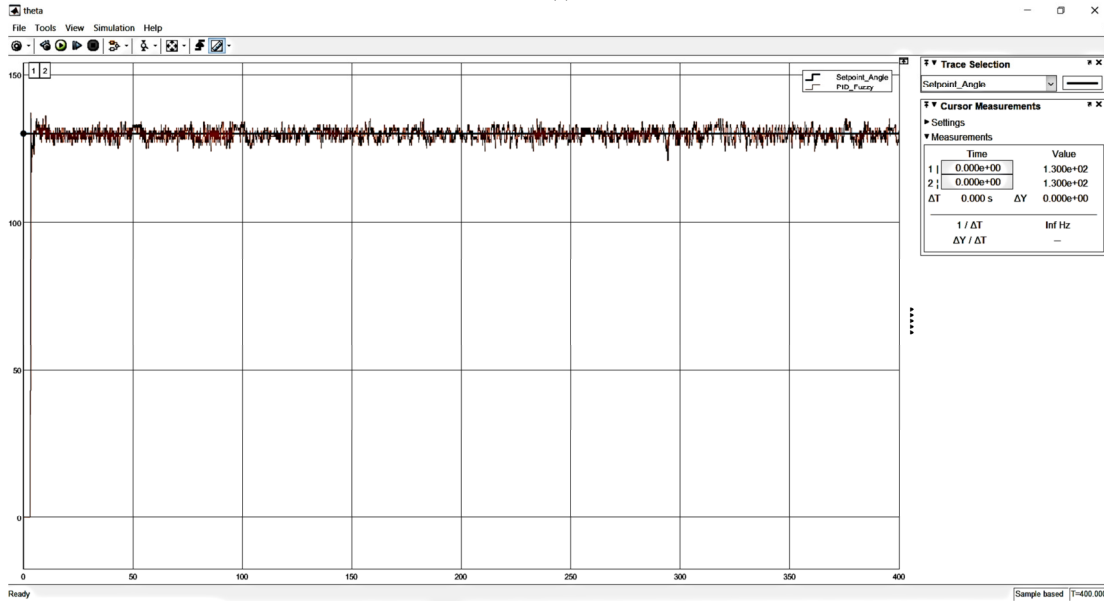
Fig. 6. Comparison of simulation results in MATLAB/Simulink for the three controllers.

The Mamdani-type FLC described in [1] exhibited a settling time of approximately 0.6 s, whereas the proposed Sugeno-type FLC demonstrated superior performance with a settling time of approximately 0.2 s and no overshoot. In contrast, the PID controller exhibited inferior control quality, including substantial overshoot, significant oscillations (though damped), and an extended settling time of approximately 1 s. Table II clearly demonstrates the advantages of the proposed Sugeno FLC, such as faster settling time, no overshoot, and superior stability compared to FLC [1] and PID controllers, validating the effectiveness of the proposed method.

After selecting the appropriate control method, the next step is to program and experiment, to demonstrate the effectiveness of the proposed PD-like FLC for the actual inverted pendulum system model, as shown in Figures 7 and 8.



(a)



(b)

Fig. 7. The actual inverted pendulum system used for this work: (a) MATLAB/Simulink to connect with the actual model and (b) representation of the experimental results.

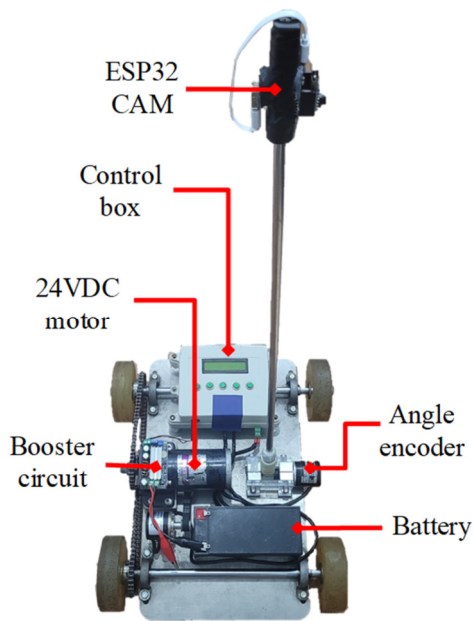


Fig. 8. Inverted pendulum system model.

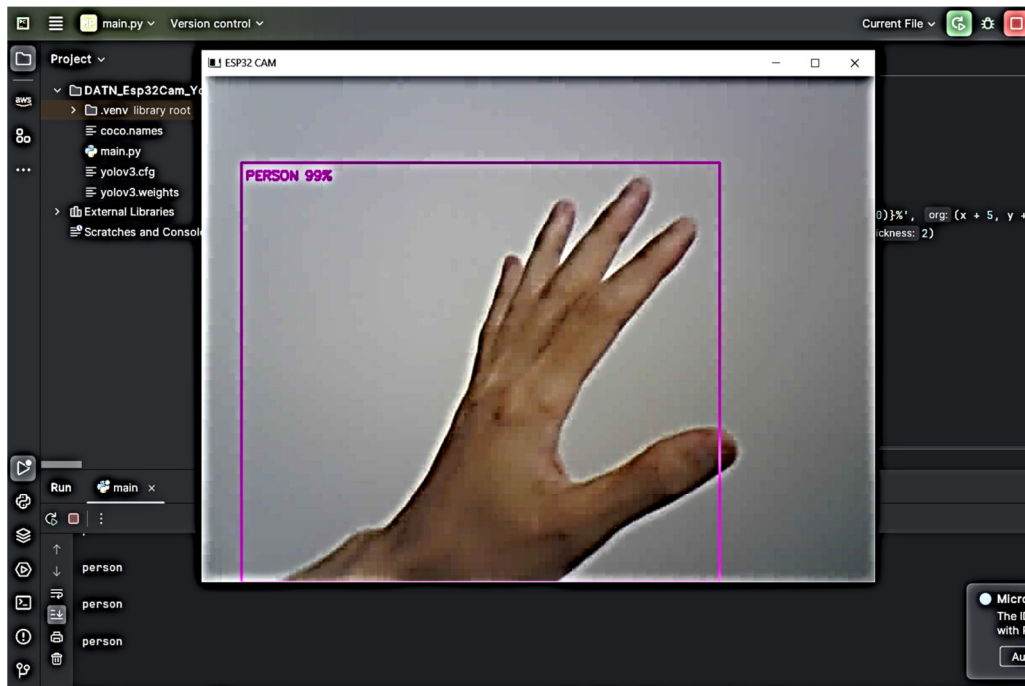
TABLE II. COMPARATIVE ANALYSIS FOR THE SIMULATION RESULTS

Controller	Steady-state error	Overshoot	Steady time	Major features
FLC [1]	Near-zero	None	~0.6 s	Relatively stable but slower than Sugeno
Proposed FLC	Zero	None	~0.2 s	Fastest, no overshoot, highest performance
PID	Significant fluctuations	Very large	~1 s	Worst, oscillation and long settling time

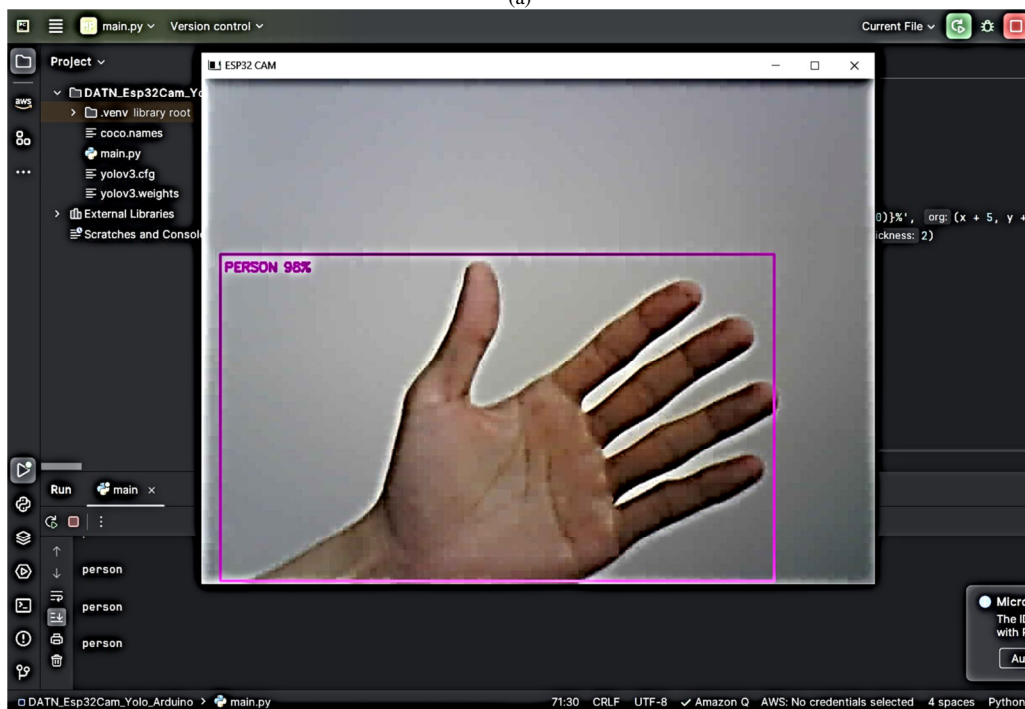
It is also noted that, after running the MGA, three scaling parameters of the proposed FLC are determined as $K1 = 4$; $K2 = 0.5$ and $Ku = 1$. Subsequently, the Arduino Mega 2560 microcontroller is programmed to communicate seamlessly with a WinForms application. This application acts as a comprehensive control and monitoring interface, responsible for receiving and displaying data transmitted by the Arduino. Furthermore, the control and monitoring interface incorporates a mechanism for displaying image data acquired from the integrated ESP32 camera module. In this study, the anticipated

data type extracted from the ESP32 CAM image data stream is classified as 'person', as shown in Figure 9. The performance of target identification and monitoring is inherently dependent on the camera sensor characteristics. The ESP32 CAM, while having moderate imaging capabilities, proves sufficient to maintain target identification and monitoring effectiveness under stable environmental conditions. However, fluctuations

in ambient illumination and increased target velocity necessitate the deployment of a higher specification camera system. This upgrade would mitigate the adverse effects of dynamic environmental changes and rapid target motion, ensuring consistent and reliable target acquisition and tracking. Figure 10 shows the monitoring results of the inverted pendulum under study using the WinForms.



(a)



(b)

Fig. 9. Image processing results obtained from ESP32 CAM.

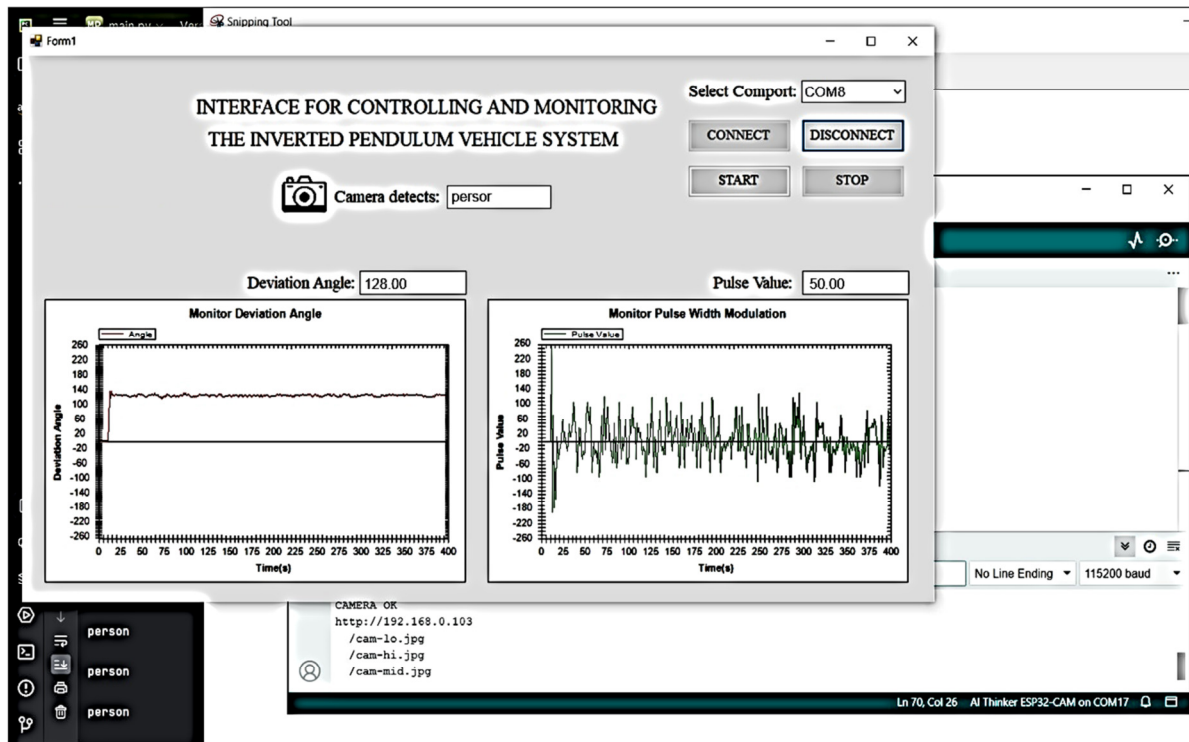


Fig. 10. Monitoring results of the entire inverted pendulum cart system on WinForms.

V. CONCLUSION

The empirical results clearly demonstrate the effectiveness of the proposed PD Fuzzy Logic Controller (FLC) in stabilizing and maintaining the pendulum's equilibrium on the vehicle. This is substantiated by the consistent convergence of the pendulum's deviation angle to its equilibrium position. Simultaneously, the system reliably captures and displays real-time image data from the ESP32 CAM, providing the users with a continuous visual representation of the immediate environment. The integration of a surveillance camera greatly enhances the operational utility of the system. This integration enables a range of capabilities, including comprehensive environmental monitoring, mobile object tracking and identification, and enhanced situational awareness. These capabilities are relevant to a range of applications, including service robotics, autonomous cargo transport, and advanced security systems. In summary, this research successfully demonstrates the design and implementation of an inverted pendulum system with dynamic equilibrium maintenance and a seamlessly integrated, robust object recognition surveillance camera. These results indicate significant potential and encourage further exploration and innovation in the field of robotics and intelligent mobile systems. Future studies will encompass rigorous testing of the inverted pendulum model over a range of operational parameters. Building upon these empirical results, the model's application will be expanded to various domains:

- Military applications will involve the integration of the model into systems for the surveillance and monitoring of military targets.

- Medical applications will explore potential applications in the medical sector, including the development of assistive devices and rehabilitation technologies.
- Autonomous systems will incorporate the model into advanced autonomous systems, such as self-driving vehicles, thereby enhancing environmental perception and control capabilities within complex operational environments, including supermarket environments.

APPENDIX

MODEL PARAMETERS AND SYMBOLS

Symbol	Meaning	Value [unit]
M	Mass of the cart	2.0 [kg]
m	Mass of the pole	0.5 [kg]
l	Length of the rod (mass omitted)	1.0 [m]
$x(t)$	Position of the cart	[m]
$\dot{x}(t)$	Velocity of the cart	[m/s]
$\ddot{x}(t)$	Acceleration of the cart	[m/s ²]
$\theta(t)$	Pendulum angle (upright position)	[rad]
$\dot{\theta}(t)$	Rotational velocity of the pole	[rad/s]
$\ddot{\theta}(t)$	Rotational acceleration of the pole	[rad/s ²]
F	Variable force exerted on the cart	[N]

REFERENCES

[1] T.-M.-P. Dao, V.-H. Pham, N.-K. Nguyen, and V.-M. Pham, "Balancing a Practical Inverted Pendulum Model Employing Novel Meta-Heuristic Optimization-based Fuzzy Logic Controllers," *International Journal of Advanced Computer Science and Applications*, vol. 13, no. 4, pp. 547–553, 2022, <https://doi.org/10.14569/IJACSA.2022.0130464>.

- [2] T.-N. Ho and V.-D.-H. Nguyen, "Model-Free Swing-Up and Balance Control of a Rotary Inverted Pendulum using the TD3 Algorithm: Simulation and Experiments," *Engineering, Technology & Applied Science Research*, vol. 15, no. 1, pp. 19316–19323, Feb. 2025, <https://doi.org/10.48084/etasr.9335>.
- [3] A. K. Yadav, P. Gaur, A. P. Mittal, and M. Anzar, "Comparative analysis of various control techniques for inverted pendulum," in *India International Conference on Power Electronics 2010*, New Delhi, India, 2011, pp. 1–6, <https://doi.org/10.1109/IICPE.2011.5728071>.
- [4] M. Rabah, A. Rohan, and S.-H. Kim, "Comparison of Position Control of a Gyroscopic Inverted Pendulum Using PID, Fuzzy Logic and Fuzzy PID controllers," *International Journal of Fuzzy Logic and Intelligent Systems*, vol. 18, no. 2, pp. 103–110, Jun. 2018, <https://doi.org/10.5391/IJFIS.2018.18.2.103>.
- [5] C. A. Ibañez, O. G. Frias, and M. S. Castañón, "Lyapunov-Based Controller for the Inverted Pendulum Cart System," *Nonlinear Dynamics*, vol. 40, no. 4, pp. 367–374, Jun. 2005, <https://doi.org/10.1007/s11071-005-7290-y>.
- [6] T. Paryono, A. Fauzi, R. A. Nanda, S. Aripriyanto, and M. Khaerudin, "Detecting Vehicle Numbers Using Google Lens-Based ESP32CAM to Read Number Characters," *MATRIK: Jurnal Manajemen, Teknik Informatika dan Rekayasa Komputer*, vol. 22, no. 3, pp. 469–480, Jul. 2023, <https://doi.org/10.30812/matrik.v22i3.2818>.
- [7] K. C. Gupta, G. Kaur, and A. Chaudhary, "Drowsiness Detection Using ESP32CAM," in *2023 3rd Asian Conference on Innovation in Technology*, Ravet IN, India, 2023, pp. 1–4, <https://doi.org/10.1109/ASIANCON58793.2023.10269977>.
- [8] A. Okubanjo and O. Oyetola, "Dynamic Mathematical Modeling and Control Algorithms Design of an Inverted Pendulum System," *Turkish Journal of Engineering*, vol. 3, no. 1, pp. 14–24, Jan. 2019, <https://doi.org/10.31127/tuje.435028>.
- [9] S. P. Dharshini D., R. Saranya, and S. Sneha, "Esp32 cam based object detection & Identification with opencv," *Data Analytics and Artificial Intelligence*, vol. 2, no. 4, pp. 166–171, Dec. 2022, <https://doi.org/10.46632/daai/24/31>.
- [10] S. Jana, R. Biswas, T. Das, K. Pal, A. Banerjee, and A. Majumdar, "Exploring Image Processing with Python," *International Research Journal of Engineering and Technology*, vol. 11, no. 02, pp. 294–297, Feb. 2024, <https://doi.org/10.13140/RG.2.2.26885.32480>.
- [11] M. Arora, P. Mangipudi, M. K. Dutta, and R. Burget, "Image Processing Based Automatic Identification of Freshness in Fish Gill Tissues," in *2018 International Conference on Advances in Computing, Communication Control and Networking*, Greater Noida, India, 2018, pp. 1011–1015, <https://doi.org/10.1109/ICACCCN.2018.8748778>.
- [12] L. B. Prasad, B. Tyagi, and H. O. Gupta, "Modelling and Simulation for Optimal Control of Nonlinear Inverted Pendulum Dynamical System Using PID Controller and LQR," in *2012 Sixth Asia Modelling Symposium*, Bali, Indonesia, 2012, pp. 138–143, <https://doi.org/10.1109/AMS.2012.21>.
- [13] K. Srikanth and G. V. N. Kumar, "Novel Fuzzy Preview Controller for Rotary Inverted Pendulum under Time Delays," *International Journal of Fuzzy Logic and Intelligent Systems*, vol. 17, no. 4, pp. 257–263, Dec. 2017, <https://doi.org/10.5391/IJFIS.2017.17.4.257>.
- [14] L. B. Prasad, B. Tyagi, and H. O. Gupta, "Optimal Control of Nonlinear Inverted Pendulum System Using PID Controller and LQR: Performance Analysis Without and With Disturbance Input," *International Journal of Automation and Computing*, vol. 11, no. 6, pp. 661–670, Dec. 2014, <https://doi.org/10.1007/s11633-014-0818-1>.
- [15] J. C. Cortes-Rios, E. Gomez-Ramirez, H. A. Ortiz-De-La-Vega, O. Castillo, and P. Melin, "Optimal design of interval type 2 fuzzy controllers based on a simple tuning algorithm," *Applied Soft Computing*, vol. 23, pp. 270–285, Oct. 2014, <https://doi.org/10.1016/j.asoc.2014.06.015>.
- [16] A. Ahmadi, H. Abdul Rahim, and R. Abdul Rahim, "Optimization of a self-tuning PID type fuzzy controller and a PID controller for an inverted pendulum," *Journal of Intelligent & Fuzzy Systems: Applications in Engineering and Technology*, vol. 26, no. 4, pp. 1987–1999, Jul. 2014.
- [17] V. Kumar and A. P. Mittal, "Parallel fuzzy P+fuzzy I+fuzzy D controller: Design and performance evaluation," *International Journal of Automation and Computing*, vol. 7, no. 4, pp. 463–471, Nov. 2010, <https://doi.org/10.1007/s11633-010-0528-2>.
- [18] A. N. K. Nasir, M. A. Ahmad, and M. F. Rahmat, "Performance Comparison Between LQR And PID Controllers For An Inverted Pendulum System," *AIP Conference Proceedings*, vol. 1052, no. 1, pp. 124–128, Oct. 2008, <https://doi.org/10.1063/1.3008655>.
- [19] Y. Liu, Z. Chen, D. Xue, and X. Xu, "Real-time controlling of inverted pendulum by fuzzy logic," in *2009 IEEE International Conference on Automation and Logistics*, Shenyang, China, 2009, pp. 1180–1183, <https://doi.org/10.1109/ICAL.2009.5262618>.
- [20] R. D. Luca, M. D. Mauro, and A. Naddeo, "The inverted pendulum," *European Journal of Physics*, vol. 39, no. 5, Aug. 2018, Art. no. 055008, <https://doi.org/10.1088/1361-6404/aad3d6>.
- [21] G. S. Maraslidis, T. L. Kottas, M. G. Tsiouras, and G. F. Fragulis, "A Fuzzy Logic Controller for Double Inverted Pendulum on a Cart," in *2021 6th South-East Europe Design Automation, Computer Engineering, Computer Networks and Social Media Conference*, Preveza, Greece, 2021, pp. 1–8, <https://doi.org/10.1109/SEEDA-CECNSM53056.2021.9566228>.
- [22] A. T. Karasahin and M. Karali, "Performance Comparison of Different Fuzzy Logic Controllers on Vehicle-Caravan Systems," *Engineering, Technology & Applied Science Research*, vol. 13, no. 4, pp. 11271–11276, Aug. 2023, <https://doi.org/10.48084/etasr.5982>.
- [23] R. Jayanth, A. M. Kumar, C. H. K. Ram, A. Manoj, G. Pavithra, and T. C. Manjunath, "Ball Detection and Tracking through Image Processing using Python," *International Journal of Engineering Technology and Management Sciences*, vol. 7, no. 4, pp. 6–10, Aug. 2023, <https://doi.org/10.46647/ijetms.2023.v07i04.002>.